Light metals 2010

THE DETERMINATION OF POT CURRENT DISTRIBUTION BY MEASURING MAGNETIC FIELDS

Nobuo Urata[1] and James W. Evans[2]

[1] Consultant and Technical Advisor, Wireless Industrial Technologies, Inc.
[2] Professor Emeritus, Dept. Matls. Sci. & Eng., University of California Berkeley and Wireless Industrial Technologies, Inc.

Keywords: Hall-Héroult cells, current efficiency, anode effect, anode current measurement, magnetic fields

Abstract

A couple of previous papers have suggested that the current distribution in a pot can be determined by measuring magnetic fields, e.g. the distribution of current among the anode rods can be found by placing a magnetic field sensor next to each rod. Because the current distribution can have a significant effect on pot performance, the suggestion is worth analyzing and this has been done by mathematical models in the present paper. One important aspect of such measurements is the effect of fields generated by other currents on the measurement of a particular current, e.g. the effect of currents in adjacent anode rods on the measurement for one rod. It is shown that, with the use of a sufficient number of sensors, it should be possible to de-convolute individual anode currents, and other currents, from the measured field values.

Introduction

For many years it has been recognized that the current efficiency of Hall-Héroult cells is dependent on anode-cathode distance. For example Grjotheim et al.[1] summarize earlier data from industrial cells in a figure similar to the more recent results of Figure 1. That figure, from the work of LeRoy and colleagues[2] on a 280kA cell, shows that the CE is fairly insensitive to ACD above a critical ACD but, below that, the CE drops sharply as the anodes are lowered, at the rate of about 0.7% per mm.

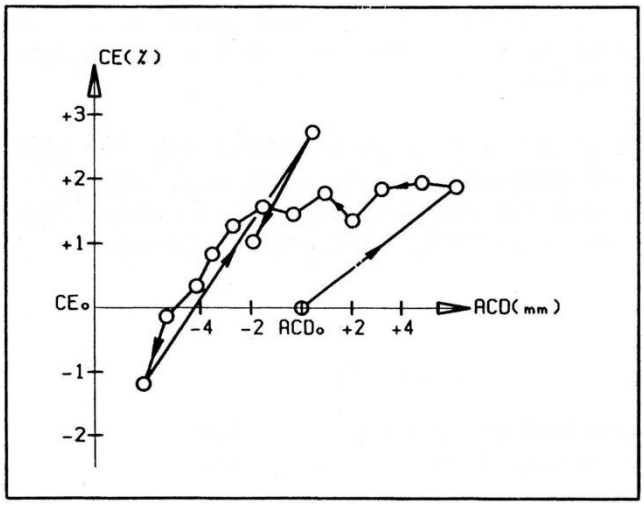

Fig. 1 Effect of anode-cathode distance on current efficiency as reported by LeRoy et al.

The evident dependence of CE on ACD can be explained in terms of enhanced re-oxidation of metal due to enhanced mass transport in the inter-polar bath resulting from additional agitation of this bath by bubbles and magnetohydrodynamic forces as the anode approaches the metal. If this is true then it follows that the CE *of an individual anode* would be impacted if that anode alone were lowered below a critical ACD. This lowering would result in excess current in that anode. It follows that a cell with one or a few anodes below the critical ACD (and the rest above) would likely have a lower overall CE than one where all anodes are above the critical ACD. Alternatively this suggests that a cell where all anodes carry the same current should have a higher CE than one where the anodes carry widely different currents. This expected decline of CE as the spread of anode currents increases appears anecdotal in the industry although we have not found a publication documenting it. We conclude that the continuous measurement of individual anode currents should give the opportunity for improvement of CE.

A second reason for measurement of individual anode currents is the opportunity that it provides for early detection of anode effects. Steingart et al.[3] have shown that wireless magnetic field sensors can readily detect the drop in current of an anode as it approaches an anode effect. The drop in current occurs several tens of seconds before the anode effect shows up in the cell voltage.

The most common method of measuring individual anode currents is by using a two point probe (sometimes known as a "banjo"), connected to a voltmeter, to measure the voltage drop down a known length of the anode rod. While convenient for development or diagnostic purposes this does not seem practical for the level of control envisioned in the present paper. Permanently attaching the voltage measurement to the anode rod is inhibited by the need to change anodes. An alternative is to measure the voltage drop across an anode flex for those cells with "pair control anodes". Unfortunately this is an unusual cell design so there exists a need for a continuous anode current measurement technique. Currents, both DC and AC, are routinely measured throughout the world by measuring the magnetic field resulting from such currents and the present paper focuses on how this could be done for the anodes of Hall-Héroult cells.

Some results of measurements on a Hydro pot are given in Figure 2. Magnetic fields were measured near the front and back of each anode rod and averaged (brown circles). Banjo measurements gave the voltage drop along a known length of each anode rod (orange triangle), i.e a measurement proportional to

each anode current. Note the close correlation between the average magnetic field and the banjo voltage measurements. Note also that both methods show the anticipated low currents in the rods of anodes that have recently been replaced.

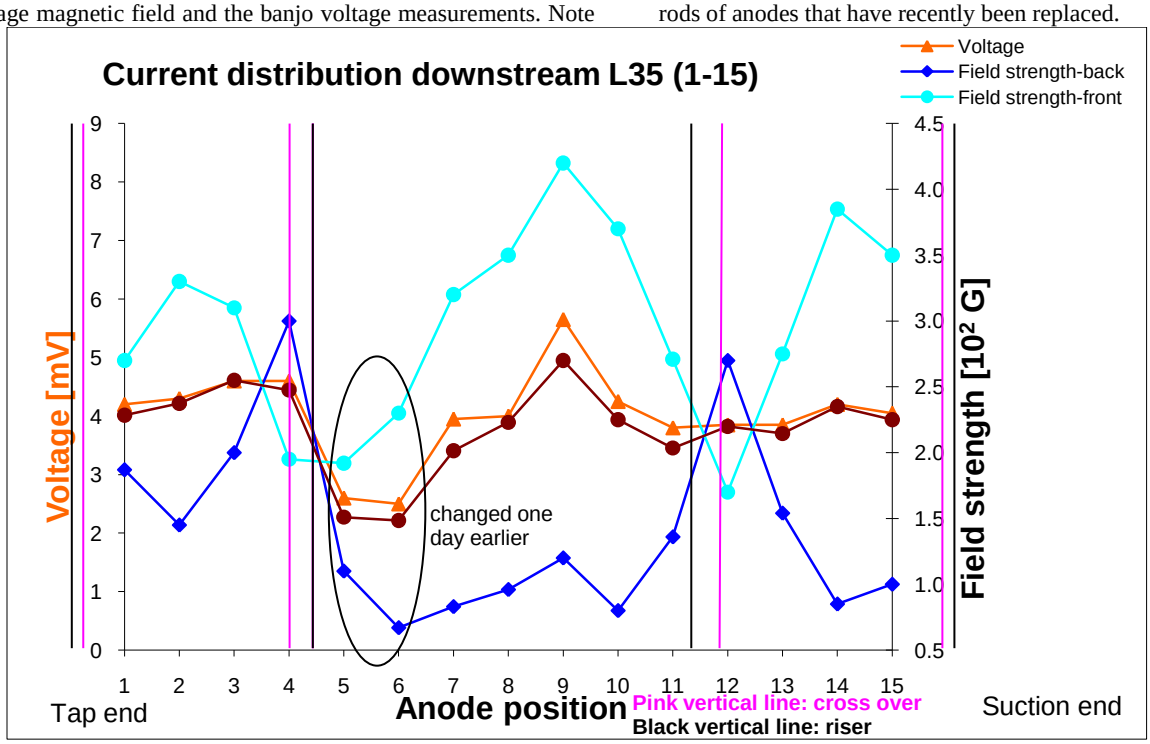

Fig. 2. Measurements of voltage drop along anode rods and magnetic fields kindly supplied by Espen Sandnes of Hydro.

Two difficulties with anode current determination by measuring magnetic fields are immediately apparent:

1. The usual reluctance to attach sensors to signal wires relaying data around the potroom to computers.
2. The contribution to the magnetic field near one anode rod from currents in other anode rods and other conductors such as cross-over bars.

Wireless transmission of data can overcome the first difficult. It has been described in a few papers[3,4,5] and will not be treated further here. The remainder of the paper describes how the second difficulty may be overcome with an approach relying on dual sensors as described in the next section. The approach is tested using two mathematical models as described under "Model results" below and conclusions drawn as to the viability of the approach.

The measurement principles

Figure 3 is a schematic diagram of two anode rods seen from above. Near each anode rod a pair of magnetic field sensors are placed to measure the field at each sensor. The magnetic field at sensors 1 and 2 is proportional to the current in anode rod 1 but it is also influenced by the current in rod 2, as well as by other current carrying parts of the pot. The field produced at sensor 1 by the current in anode rod 1 is significantly greater than that produced at sensor 2. The current in anode rod 2 produces a much weaker field at sensors 1 and 2; furthermore anode rod 2 gives almost the same field at sensors 1 and 2 so that by subtracting the two sensor readings we can almost eliminate the effect of anode rod 2. Thus the simplest method of obtaining the current is to subtract the sensor readings from each other and multiply by a calibration constant. Below this is referred to as the "simple method".

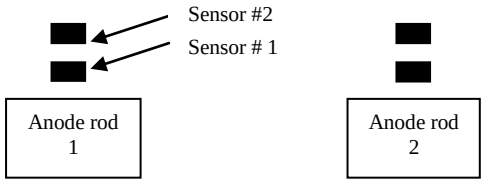

Fig. 3. Schematic diagram of two anode rods (from above) and two pairs of magnetic field sensors.

Table 1. Various computed contributions to the magnetic field at two sensors near anode rod # 3.

Magnetic field (gauss) at two sensors near anode rod #3 due to currents in:	Sensor #1	Sensor #2
anode rod #3	175	162
anode rod #2	0.305	0.335
cross-over bar adjacent to rod #3	7.15	7.19
riser adjacent to rod #3	8.37	8.39

Table 1 illustrates some of the points from the preceding paragraph. These are the results of calculations detailed in the next section on the magnetic fields arising from currents in the anode rods etc of a representative cell. Evidently the field experienced by the pair of sensors next to the rod of anode #3 is largely due to the current in that rod. The

contribution from the current in an adjacent anode (#2) is small by comparison and its contribution to the difference between the field at the two sensors (0.335-0.305 = 0.03) is very small compared to the difference between the contributions from current in anode rod #3 (175-162 = 17). Contributions from currents in cross-over bars and risers (that are next to anode #3) are not small but yet again the *differences* between the contributions at the two sensors (7.19-7.15 = 0.04 and 8.39-8.37 = 0.02 respectively) are very small. The values in Table 1 are field components in the long horizontal direction of the cell. The anode bus runs in this direction so currents in this bus should not contribute to the sensor readings.

An even more precise procedure is to correct the results from the sensor readings for anode rod 1 using the sensor readings for anode rod 2 (and all other anode rods and other accessible conductors where sensor (pairs) can be placed) and *vice versa*. This is the essence of what we call the "many sensor method" below; the correction is achieved by solving a set of simultaneous equations giving the field at each sensor as the sum of contributions from all currents nearby. The coefficients in these equations are obtained from an analytical equation relating the field at a point near a conductor of finite dimensions carrying unit current; the equation is too lengthy for reproduction here.

Testing of methods using mathematical models

The methods for determining current from magnetic field measurements were tested using two mathematical models. The first of these models ("superstructure model") employs analytical equations to rapidly compute magnetic fields arising from specified currents in risers, cross-over bars and anode rods (leaving out the anode bus as its fields are not in the long horizontal direction that is under study here). This model lends itself readily to the inverse calculation where all currents are calculated from specified (e.g. measured) magnetic fields. The model neglects currents in the anodes, bath and lower in the expectation that they make a negligible contribution to the *differences* between each of the sensor pairs in the superstructure. The model was used to test both the simple method and the many sensor method described in the previous section.

The second model was an updated version of the model described by Urata and colleagues[6]. It is a model of the whole cell (and allowing for field contributions from nearby cells) that calculates all important cell variables such as the voltage and current distributions, magnetohydrodynamics etc. This model was used to test only the simple method of deducing currents from field measurements; below it is referred to as the "full model".

Model results

Testing using the superstructure model

Figure 4 illustrates the superstructure used in the superstructure model.

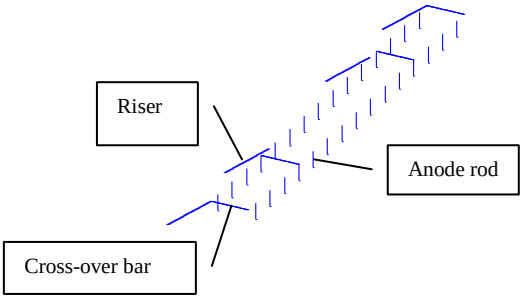

Fig. 4 Schematic diagram of the conductors in the superstructure model.

The cell to which this superstructure belongs is a fictional one although dimensions etc, have been chosen to be representative of real cells. Although the three types of conductors are represented as lines in Figure 3, the calculations were done with conductors of finite width, thickness and length.

First the model was used to calculate magnetic fields at the sensor locations with all conductor currents specified (e.g. all anode rod currents set to 10,000 amps) and as if all conductors above had a sensor pair mounted next to them. Then the computed fields were used to calculate the currents in all the conductors, first using the simple method (anode current calculated only from fields at its sensor pair) and then by the many sensor method (anode current calculated from readings of all sensor pairs). Naturally the latter yields the currents that we started with, to within the precision of the numerics. The results appear in the first row of numbers in Table 2. It is seen that the simple method yields a mean error in the anode current of 1.9% although one of the currents is off by 10.2%. The simple method therefore has its limitations.

Table 2. Calculated % error in determining current from magnetic field in model calculations. All anodes at 10kA.

Included in calculation:	**Simple method**		**Many sensor method**	
	Mean % error	Max % error	Mean % error	Max % error
whole superstructure	1.9	10.2	"Exact"	"Exact"
anode rods & cross-overs	1.9	10.2	0.35	0.83
only anode rods	1.9	10.2	1.9	10.0

Then the calculations of current were repeated for both methods but with sensor "data" from sensors next to risers left out. The results appear in the second row of numbers. The simple method yields the same errors as before but now the many sensor method has error (due to the currents in the risers being inaccessible); however these errors appear reasonable with a maximum value of 0.83%.

Finally the sensor "data" for both risers and cross-over bars was left out of the calculations. Now the errors from the many sensor method are hardly better than those from the

simple method. The practical implication is that sensors near the risers are probably not necessary but that there should be sensors near the cross-overs (as well as the anode rods).

The calculations just described were then repeated for a very skewed anode current distribution (anode #3 being at 20,000amps with the other anodes at 10,000amps). In terms of the % error the results were not significantly different from those of Table 2. Figure 5 shows the current distribution for this skewed current distribution case as calculated by the simple method. Although the 20kA of anode #3 is accurately captured there are significant errors for anodes 2,4 and 12, together with lesser errors in 1 and 15, probably because of the nearby cross-overs.

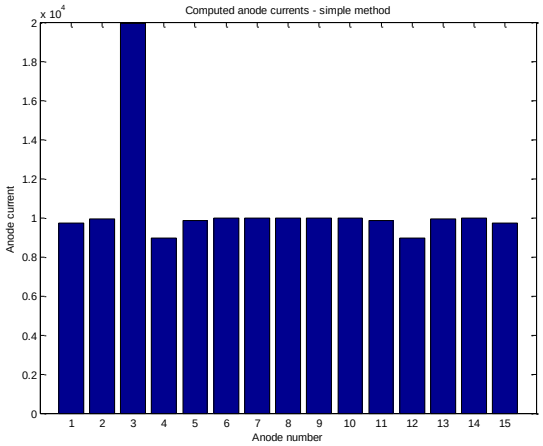

Fig. 5. Current distribution among anodes for skewed current distribution calculated by simple method. Except for anode #3 currents should be 10kA. Only one of anode rows shown.

Currents, for the same skewed distribution, as calculated by the many sensor method appear in Figure 6. The anode rods and cross-overs were included in the calculation, but not the risers.
The superiority of the many sensor method is evident.

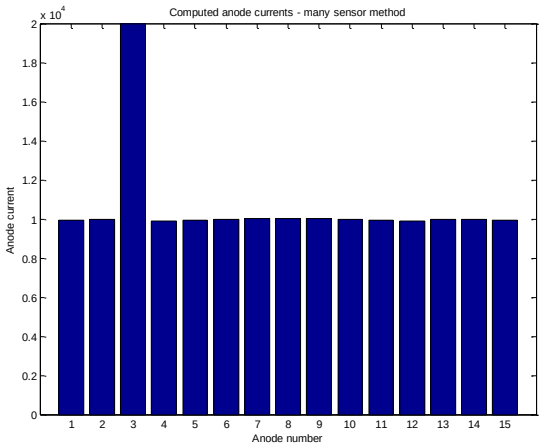

Fig. 6. Current distribution among anodes for skewed current distribution calculated by many sensor method. Except for anode #3 currents should be 10kA. Only one of anode rows shown.

Testing using the full model

For evaluating the accuracy of the method, proposed in this article, a cell equipped with a commercial type busbar-system and the lining was modeled. This cell has 16 anodes and the amperage is 230 kA with two end and two quarter risers. Because a tight room-to-room distance is considered, an asymmetric bus arrangement has been incorporated in the design. The anode/rod numbering is shown in Figure 7.

Anode/Rod numbering	Downstream								
Center	1	2	3	4	5	6	7	8	Window
Aisle	9	10	11	12	13	14	15	16	side
	Upstream								

Fig. 7. Numbering system of anodes used in the full model.

Using the model and specifying the anode-cathode-distance under each anode, we computed the anode currents (anode currents from the MODEL) and the magnetic fields near the anode rods. To study the effects of the different anode currents, such as perfectly even distribution or one anode overloading, we assumed the different ACDs. Then, using the computed magnetic fields, we projected the anode currents (anode current from the MAGNETIC FIELDS). Thus, an assessment is made about how well we can predict the anode current distribution from the magnetic field near the rods. Note that the component of the magnetic field in the long horizontal direction of the cell is the one under examination here and this field was calculated at the two sensor locations next to each anode rod.

Table 3. CASE-1 Uniform Anode Cathode Distance

A	B	C	D	E
Anode #	CURRENT Model	M-Index	CURRENT Projected	Error
	amperes	Gauss	amperes	%
1	14,339	42.7	14,686	2.4
2	14,330	40.8	14,033	-2.1
3	14,306	40.8	14,033	-1.9
4	14,267	42.2	14,514	1.7
5	14,268	42.2	14,514	1.7
6	14,309	40.8	14,033	-1.9
7	14,336	40.9	14,067	-1.9
8	14,352	42.7	14,686	2.3
9	14,433	43.1	14,814	2.6
10	14,454	40.9	14,058	-2.8
11	14,445	41.2	14,161	-2.0
12	14,405	42.5	14,614	1.5
13	14,405	42.5	14,618	1.5
14	14,444	41.3	14,215	-1.6
15	14,459	41.1	14,129	-2.3
16	14,448	43.1	14,824	2.6
average	14,375	41.8		

The difference between the two fields is called the M-Index in the table above and what follows. The current in each rod was then projected from the M-Index by what is essentially the simple method described above.

First, assuming the uniform anode cathode distance, both the anode /rod current distribution (CURRENT Model - column B) and the M-Index (column C) were calculated as shown in the Table 3 (CASE-1).

In CASE 1, column D shows the prediction of the rod current based on the M-Index (column C).
The calculation is made as follows:

Rod current = [Rod M-Index] / [Average M-Index] * 14,350

Note that 14,350 is [230,000/16], the nominal current for each anode at 230 kA load. Note also,

[Average M-Index] = 41.8 (from table).

The rod currents based on the M-Index are similar to the rod currents from the model. The results are compared in Column E as relative error percentages. Column E shows that the prediction based on the M-Index is very reliable and the disturbing effect of the other currents on the accuracy is not large.

Next, assuming a current-overload over the upstream corner anode (#16), we re-evaluated the accuracy. The corner anode was assumed to have roughly 30% less anode-cathode-distance. Table 4 shows the results (CASE 2).The #16 anode shows 19kA while the other anodes carry 14 kA. The projected currents based on the M-Index are shown in Column D. The #16 current is projected to be 19.6 kA compared to 19.0 kA in the model. The relative errors are shown in E. In addition, as shown in Column F, the error percentage is significantly reduced when the error % in CASE 1 is subtracted.

Table 4. CASE-2 Corner Anode Overloaded (upstream #16 anode)

A	B	C	D	E	F
Anode/ rod #	CURRENT Model	M-Index	CURRENT Projected	Error	Corrected error
	ampere	Gauss	ampere	%	%
1	14,055	41.8	14,376	2.2	-0.2
2	14,044	40.0	13,756	-2.0	0.1
3	14,017	39.9	13,722	-2.1	-0.2
4	13,974	41.3	14,204	1.6	-0.1
5	13,969	41.2	14,169	1.4	-0.3
6	14,003	40.0	13,756	-1.7	0.2
7	14,025	40.0	13,756	-1.9	0.0
8	14,035	41.9	14,410	2.6	0.3
9	14,144	42.2	14,510	2.5	-0.1
10	14,163	40.0	13,757	-2.8	-0.1
11	14,148	40.3	13,853	-2.0	-0.1
12	14,100	41.6	14,296	1.4	-0.1
13	14,089	41.5	14,286	1.4	-0.1
14	14,113	40.3	13,856	-1.8	-0.2
15	14,108	39.8	13,702	-2.8	-0.5
16	19,012	57.0	19,589	4.0	1.4
average	14,375	41.8			

A similar calculation, CASE 3, was tried for the case of overloading the #14 anode/rod, which is located close to the quarter riser. Each quarter riser carries roughly 40% of the line current, possibly creating an error in the current calculation. In this case, however, the M-Indices led to the result better than CASE-2. The error correction based on CASE-1 again reduced the errors considerably.

Analyzing the results from the full model

First, the effect of the risers is analyzed. The result shows that the maximum effect is 0.1 gauss, a negligible amount, created by the right side quarter riser (in CASE 2 of the #16 corner anode overload). Thus, the disturbance from the risers can be neglected.

Table 5 shows the contribution of the currents from the adjacent anodes/rods. The #16 overload case is shown in Column B and C. The contribution of the other anode/rods (#5 to #8 and #13 to #15), affecting on the #16 M-Index, is seen. The contribution pattern shows that an adjacent anode on the upstream (same side) and the facing anodes on the next row (the other side) mostly affect the M-Index of #16. Their contribution is not serious but probably needs to be considered in the actual implementation, for example by using the many sensor method mentioned above.

The #14 overload is shown in Column D and E. Since #14 is the internal anode (not located at the cell-end), two adjacent anodes (#13 and #15) on the upstream side affect the M-Index and three facing anodes (#5,#6 and #7) also has some impact.

Table 5. Effect of the Adjacent Rods

	#16 overloading		#14 overloading	
A	B	C	D	E
Rod#	Rod Current	M-Index	Rod Current	M-Index
	ampere	Gauss	ampere	Gauss
Downstream				
5	13,969	0	13,969	0.1
6	14,003	0	14,005	0.3
7	14,025	0.1	14,031	0.1
8	14,035	0.2	14,046	0
Upstream				
13	14,089	-0.1	14,074	-0.5
14	14,113	-0.1	**19,047**	**43.8**
15	14,108	-0.5	14,122	-0.5
16	**19,012**	**43.8**	14,117	-0.1

Note: 1 Gauss = 10^{-4} Tesla

It is shown that the accuracy of the current prediction based on the M-Index is satisfactory when compared to the traditional methods of either embedding the lead wires or manually measuring the mV drops by banjo. In addition, when the correction is applied to each reading, the accuracy improves significantly and the error percentage remains below 1%.

Conclusions

The model computations demonstrate that the proposed determination of anode currents, by measurement of the magnetic field at two positions adjacent to each anode rod, can predicts the rod currents, even without considering the impact of the other

current elements. However, when the interference from the other current elements is taken into account, the accuracy becomes so excellent that this could represent the next generation of future cell operation. Accurate rod current monitoring will reveal the very subtle and early changes in the inter-polar area under every anode, definitely leading to a significant improvement in the operational efficiency.

---

[1] K. Grjotheim, C. Krohn, M. Malinovský, K. Matiašovský and J. Thonstad, "Aluminum Electrolysis; The Chemistry of the Hall-Héroult Process", Aluminium-Verlag, Düsseldorf, 1977

[2] M. J. LeRoy, T Pelekis and J-M Jolas, " Continuous Measurement of Current Efficiency, by Mass Spectrometry, on a 280 kA Prototype Cell", "Light Metals 1987", p291, R. D. Zabreznik ed., TMS, Warrendale, PA, 1987.

[3] D. Steingart, J. W. Evans, P. Wright and D. Ziegler, "Experiments on Wireless Measurement of Anode Currents in Hall Cells", "Light Metals 2008", p333, R. Peterson ed., TMS, Warrendale, PA 2008

[4] M. Schneider, J. W. Evans, P. Wright and D. Ziegler, "Further Results from Wireless Instrumentation of Hall-Héroult Cells" "Light Metals 2006", p 331, T. J. Galloway ed., TMS, Warrendale, PA (2006).

[5] M. H. Schneider, J. W. Evans and P. K. Wright, "Designing a thermoelectrically powered wireless sensor network for monitoring aluminium smelters", Proc. Instn. Mech. Engrs., Part E: J. of Process Mech. Eng., vol 220, #3 (2006), p181

[6] H. Q. Tang, N. Urata, C. M. Read and S. L. Stejer, "Response of Hall-Héroult Cell to Step Changes in Operating Conditions: Measurements and "Dynamic" Simulations", "Light Metals 1998", p349, B. J. Welch ed., TMS, Warrendale, PA, 1998